

Oncolytic HSV and Erlotinib Inhibit Tumor Growth and Angiogenesis in a Novel Malignant Peripheral Nerve Sheath Tumor Xenograft Model

Yonatan Y Mahller^{1,2,3,4}, Sachin S Vaikunth^{2,5}, Mark A Currier¹, Shyra J Miller², Maria C Ripberger^{2,5}, Ya-Hsuan Hsu⁶, Ruty Mehrian-Shai⁶, Margaret H Collins⁷, Timothy M Crombleholme^{2,5}, Nancy Ratner² and Timothy P Cripe^{1,2}

¹Division of Hematology/Oncology, Cincinnati Children's Hospital Medical Center, Cincinnati, Ohio, USA; ²Division of Experimental Hematology, Cincinnati Children's Hospital Medical Center, Cincinnati, Ohio, USA; ³Physician Scientist Training Program, University of Cincinnati College of Medicine, Cincinnati, Ohio, USA; ⁴Graduate Program of Molecular and Developmental Biology, University of Cincinnati College of Medicine, Cincinnati, Ohio, USA; ⁵Department of Pediatric General, Thoracic, and Fetal Surgery, Cincinnati Children's Hospital Medical Center, Cincinnati, Ohio, USA; ⁶Division of Biochemistry and Molecular Biology, Institute for Genetic Medicine, University of Southern California, Los Angeles, California, USA; ⁷Division of Pathology, Cincinnati Children's Hospital Medical Center, Cincinnati, Ohio, USA

Malignant peripheral nerve sheath tumors (MPNSTs), driven in part by hyperactive Ras and epidermal growth factor receptor (EGFR) signaling, are often incurable. Testing of therapeutics for MPNST has been hampered by lack of adequate xenograft models. We previously documented that human MPNST cells are permissive for lytic infection by oncolytic herpes simplex viruses (oHSV). Herein we developed and characterized a xenograft model of human MPNST and evaluated the antitumor effects of oHSV mutants (G207 and hrR3) and the EGFR inhibitor, erlotinib. Additive cytotoxicity of these agents was found in human MPNST cell lines, suggesting that EGFR signaling is not critical for virus replication. Mice bearing human MPNST tumors treated with G207 or hrR3 by intraperitoneal or intratumoral injection showed tumor-selective virus biodistribution, virus replication, and reduced tumor burden. oHSV injection demonstrated more dramatic antitumor activity than erlotinib. Combination therapies showed a trend toward an increased antiproliferative effect. Both oHSV and erlotinib were antiangiogenic as measured by proangiogenic gene expression, effect on endothelial cells and xenograft vessel density. Overall, oHSVs showed highly potent antitumor effects against MPNST xenografts, an effect not diminished by EGFR inhibition. Our data suggest that inclusion of MPNSTs in clinical trials of oHSV is warranted.

Received 8 January 2006; accepted 25 August 2006.
doi:10.1038/sj.mt.6300038

INTRODUCTION

Neurofibromatosis type 1 (NF1) is a tumor predisposition syndrome including benign (neurofibromas) and malignant

tumors. The majority of NF1-related mortality is due to malignant peripheral nerve sheath tumors (MPNSTs).¹ Conventional chemotherapy and radiation are relatively ineffective for MPNSTs,² and patients with NF1 are at increased risk of therapy-induced malignancies.³ Surgical resection is the mainstay of treatment but survival rates remain poor.² In contrast to sporadic cases, NF1-associated MPNSTs develop earlier in life, are more aggressive and possess inherently hyperactive Ras secondary to loss of neurofibromin.² As intracellular signaling of Ras and epidermal growth factor receptor (EGFR) underlie the pathogenesis of MPNSTs,^{4,5} these signaling pathways represent potential therapeutic targets.

By Oncolytic viral vectors are being pursued as non-mutagenic anticancer therapies.⁶ As these engineered viruses harbor mutations in genes necessary for virus replication within untransformed cells, their normal (infectious) virulence is attenuated. A main advantage of oncolytic viruses is their ability to replicate selectively within tumor tissue, thereby amplifying the initial dose. Oncolytic herpes simplex virus (oHSV) mutants have demonstrated robust antitumor efficacy against preclinical cancer models⁷⁻⁹ and phase I/II clinical trials have demonstrated tumor-selective virus replication with only mild toxicities.¹⁰ The most commonly used oHSV mutants are defective for the viral neurovirulence gene encoding ICP34.5. Tumor selective targeting by ICP34.5^{-/-} oHSV is thought to be governed by levels of active Ras, that inhibits interferon-mediated antiviral host responses,¹¹ but recent reports have suggested that alternative signaling pathways such as PI3-kinase may also serve this function.¹² We previously reported that MPNST cell lines with both high and low basal Ras activity are sensitive to lytic infection by oHSV mutants.¹³ These data suggest that dysregulation of a cadre of intracellular signaling pathways may confer sensitivity to oHSV and that oHSV may be effective for cancers aside from those that rely upon hyperactive Ras.

Correspondence: Timothy P Cripe, Division of Hematology/Oncology ML7015, 3333 Burnet Ave, Cincinnati, Ohio 45229, USA.
E-mail: timothy.cripe@cchmc.org

Signaling through the EGFR pathway is well documented in many human malignancies,¹⁴ and a number of inhibitors are being studied as anticancer agents. The EGFR tyrosine kinase inhibitors gefitinib and erlotinib have shown antitumor efficacy against several human malignancies.^{15–19} Although erlotinib failed to show efficacy for patients with refractory MPNSTs in one phase II trial,²⁰ its effects in newly diagnosed patients or in combination with other anticancer therapies remain unclear.

Here, we report the development and characterization of clinically relevant subcutaneous (s.c.) and intraperitoneal (i.p.) xenograft models of human MPNST. We used the xenograft models to investigate the therapeutic effects of oHSV and erlotinib, alone and in combination. We found a significant antitumor effect with intratumoral (i.t.) or i.p. oHSV injection though only a modest antitumor activity with erlotinib. Despite additive inhibition of growth of cultured cells, *in vivo* combination therapies showed only a trend toward less tumor burden. Both oHSV and erlotinib were antiangiogenic as measured by several *in vitro* and *in vivo* parameters.

RESULTS

Generation of a xenograft mouse model of human MPNST

Human MPNST cell lines injected into immunodeficient mice s.c. required at least 3 months to develop tumors except STS26T where tumor formation occurred by day 14 (**Supplementary Table S1**). I.p. inoculated mice died by ~35 days post-injection. STS26T MPNST xenografts were highly vascular (**Figure 1a**) and showed characteristics of human disease including spindle shaped cells and abundant collagen fiber deposition (**Figure 1b** and **c**). Immunohistochemistry (IHC) illustrated focal positivity for Schwann cell/neuroendocrine markers (S100 and synaptophysin) and membranous staining for EGFR (**Figure 1d–f**).

By comparing of gene expression in primary MPNSTs, human MPNST cell lines and normal human Schwann cells (NHSCs), we previously identified a MPNST gene expression signature consisting of 159 genes.²¹ To validate the xenograft model, we evaluated the expression of these genes in STS26T cells and xenografts. Expression of a majority (72%) of MPNST signature genes was dysregulated in STS26T xenograft tumors relative to NHSC (**Figure 1g**; **Supplementary Table S2**). Several genes of known functional significance in MPNST pathogenesis were coordinately regulated between MPNST primary tumors and STS26T xenografts. For example, upregulation of neural crest transcription factors, TWIST1 and SOX9, support maintenance of a stem-like phenotype. Downregulation of mature Schwann cell markers, including NGFR and PMP22, are characteristic of abnormal differentiation. These results suggest that the STS26T xenograft model closely emulates human MPNST tumors, making it a suitable model for the testing of novel therapeutics.

Tumor selective oHSV biodistribution and replication within MPNST xenografts

To determine the systemic biodistribution of virus-mediated gene transfer, we examined i.p. tumor and normal tissues for

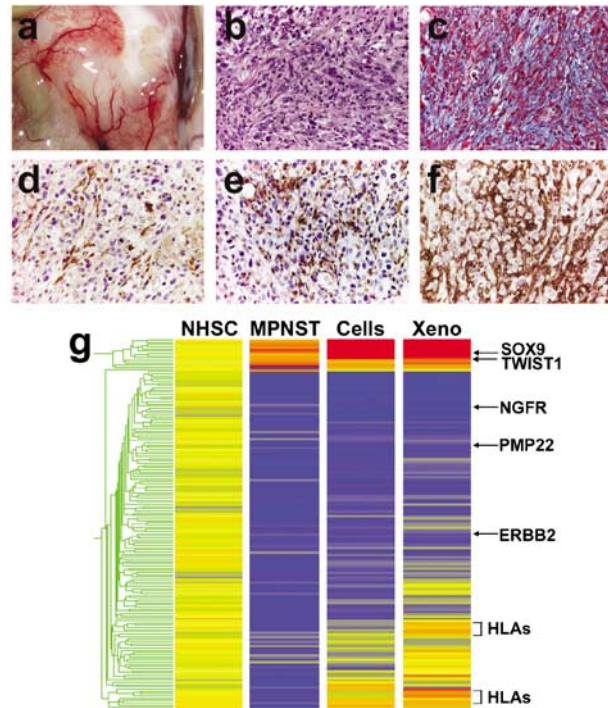


Figure 1 Characterization of MPNST xenograft models. **(a)** Large blood vessels seen surrounding an i.p. tumor nodule. **(b)** Haematoxylin and eosin (H&E) staining showing a high mitotic index and collagen fibers. **(c)** Trichrome staining revealing an abundance of extracellular matrix protein (blue). **(d)** S100, **(e)** Synaptophysin, and **(f)** EGFR IHC staining of MPNST xenografts. **(g)** Analysis of MPNST signature gene expression relative to NHSCs, primary MPNSTs, STS26T cells in culture and the MPNST xenograft model.

β -galactosidase activity following i.p. injection of phosphate-buffered saline (PBS) or hrR3 (1×10^7 plaque forming units (PFU)). Whereas normal organs from oHSV-infected mice showed no change in enzymatic activity above PBS-treated mice, tumor homogenates from oHSV-treated mice showed a 245- and 29-fold increase in β -galactosidase activity at days 3 and 7, respectively (**Figure 2a**). Thus, i.p. administration of oHSV results in tumor-selective targeting of gene expression by day 3 and at least until day 7 post-virus administration.

To determine if MPNST xenografts support virus replication, s.c. tumors ($\sim 500 \text{ mm}^3$) were infected with a single i.t. dose of G207 or hrR3 (5×10^6 PFU). Tumors injected with hrR3 contained infectious virus at all time points tested, whereas tumors infected by G207 showed detectable infectious virus only at 6 h and 48 h post-infection (**Figure 2b**). Tumors infected by either virus showed tissue destruction that stained positively for HSV antigen and contained inclusion bodies characteristic of HSV infection (**Figure 2c–e**). HSV antigen positive areas were also positive for HSV DNA by *in situ* hybridization (**Figure 2f**). Consistent with our virus replication data, HSV staining of hrR3-infected tumors contained HSV positive foci at all time points tested up to 7 days post-infection, while G207-infected tumors lost positive staining within 4 days (data not shown).

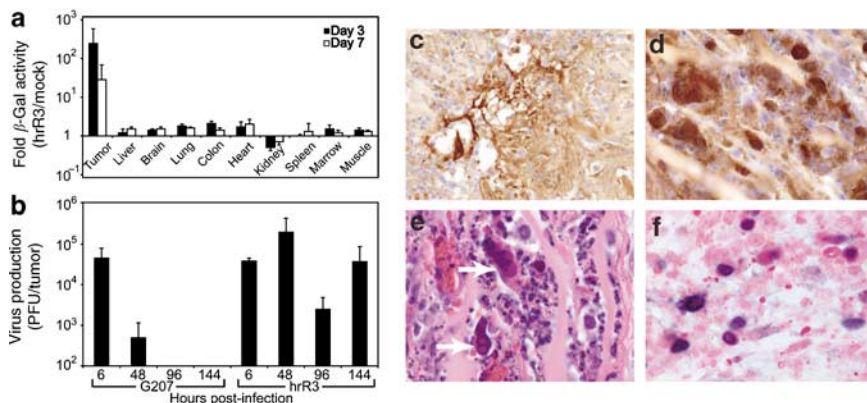


Figure 2 *In vivo* effects of oHSV treatment on MPNST xenografts. **(a)** Systemic biodistribution of HSV delivered β -galactosidase activity following i.p. administration of hrR3 (1×10^7 PFU) at 3 (■) and 7 (□) days post-infection. **(b)** Quantification of infectious HSV particles within MPNST xenografts ($\sim 500 \text{ mm}^3$) treated with a single injection of 5×10^6 PFU at hour 0 and analyzed at times shown post-infection. Microscopic analysis of hrR3-infected tumors at 48 h post-infection showed **(c)**, (original magnification $\times 200$); **(d)**, (original magnification $\times 1,000$) tissue necrosis in areas of positive HSV immunostaining, **(e)**, (original magnification $\times 1,000$) HSV inclusion bodies (white arrows) upon H&E staining and **(f)**, (original magnification $\times 1,000$) nuclear staining for HSV DNA detected by *in situ* hybridization.

oHSV treatment decreases i.p. MPNST xenograft tumor burden

To evaluate the antitumor efficacy of oHSV, mice bearing i.p. MPNST xenografts were administered three i.p. doses of PBS G207 or hrR3 (1×10^7 PFU/dose) and euthanized at day 30 or followed for survival (Figure 3a). By day 30, PBS-treated mice developed severe ascites, were less active and contained a large tumor burden. Grossly, oHSV-treated mice contained drastically reduced i.p. tumor burden relative to controls (Figure 3b). Compared with PBS-treated animals, mice injected with G207 or hrR3 contained fewer tumor nodules ($P < 0.02$, $P < 0.02$, respectively) and less tumor weight ($P = 0.12$, $P < 0.02$, respectively) (Figure 3c). Animals receiving lower doses of G207 or hrR3 showed modest reductions in tumor burden illustrating a dose-dependent oHSV effect. In a separate control experiment, animals bearing i.p. MPNST xenografts were administered three i.p. doses of PBS or UV-inactivated hrR3 (1×10^7 PFU/dose). At day 30 post-inoculation there was no difference in tumor burden between these groups (data not shown).

To determine if oHSV could affect overall survival of tumor bearing mice, i.p. inoculated animals received three i.p. injections of PBS, G207 or hrR3 (1×10^7 PFU/dose) and were followed for survival. While the median overall survival of control animals was 35 days, G207 and hrR3-treated groups survived 42 and 44 days, respectively (Figure 3d). These results correspond to a 20 and 26% prolongation of mean overall survival for G207 ($P < 0.045$) and hrR3 ($P < 0.003$) treated groups, respectively.

Although oHSV significantly reduced overall tumor burden, animals treated with the oHSV still contained tumor. To investigate potential mechanisms of tumor cell escape we examined remaining tumor nodules for β -galactosidase activity, infectious virus and for cellular resistance to oHSV. Tumor nodules recovered from G207 or hrR3-treated mice showed no β -galactosidase activity above baseline and were negative for infectious virus (data not shown). To determine if these tumors had acquired resistance to lytic infection by oHSV, cell lines were

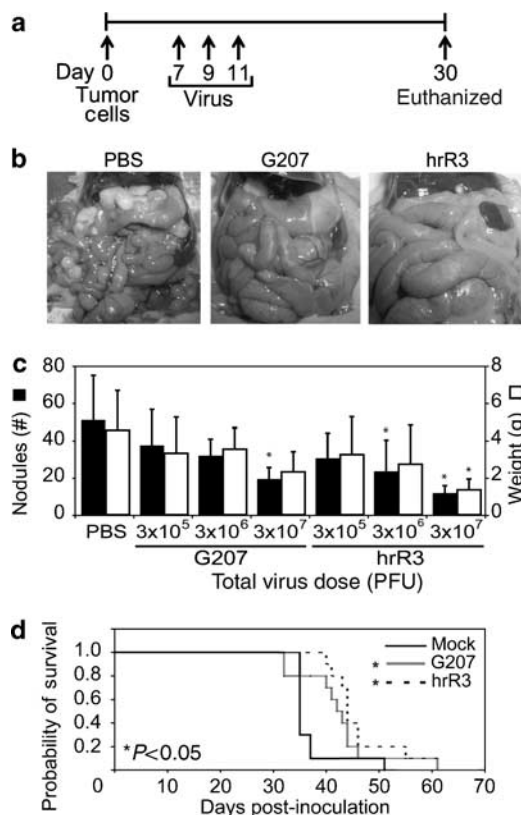


Figure 3 oHSV treatment decreases i.p. MPNST xenograft tumor burden. **(a)** Treatment regimen schematic showing i.p. injection with 4×10^6 STS26T human MPNST cells followed by i.p. oHSV administration of 1×10^5 , 1×10^6 , or 1×10^7 PFU/dose on days 7, 9, and 11. Animals were euthanized and tumor burden was evaluated at day 30 by **(b)** gross examination and **(c)** quantification of tumor nodule count (■) and total weight (□), standard deviation as shown, $n = 8$ ($*P < 0.05$). **(d)** Mice bearing i.p. tumors were treated with three doses of PBS (solid line), G207 (faded solid line) or hrR3 (dashed line) at 10^7 PFU/dose and followed for overall survival, $n = 8$ ($*\text{log-rank } P < 0.05$).

established from recovered tumor nodules. Cell lines from PBS- or virus-treated mice showed similar sensitivity to the parental cell line STS26T (data not shown). Taken together our results

suggest that oHSV are effective against MPNST xenografts, and that virus clearance may limit overall effectiveness.

oHSV mutants are antiangiogenic *in vitro* and *in vivo*

In addition to direct tumor cell lysis, others have reported oHSV effects upon tumor neovasculature.^{22,23} To investigate antiangiogenic activity against MPNST xenografts, we evaluated oHSV effects on both cultured endothelial cells and tumor vascular density. Early passage, rapidly dividing human umbilical vein endothelial cells (HUVECs) infected by G207 or hrR3 were efficiently euthanized (Figure 4a), supported robust virus replication on par with wtHSV-1 KOS (Figure 4b) and showed morphologic changes characteristic of HSV-infected cells (Figure 4c and d). To assess antiangiogenic effects of oHSV *in vivo*, s.c. MPNST xenografts (~500 mm³) were treated with a single injection of PBS or oHSVs (5 × 10⁶ PFU) and stained by IHC to identify tumor blood vessels. At one week post-infection, when tumors were still similar in size, oHSV-treated tumors showed a reduction in tumor vascular density (P<0.05) (Figure 4e). Finally, we found that following i.t. injection, oHSV could directly infect endothelial cells *in vivo* as illustrated by positive HSV staining found within rare tumor vessels (Figure 4f). Thus, oHSVs exert antitumor effects in part via reduction of tumor neovasculature.

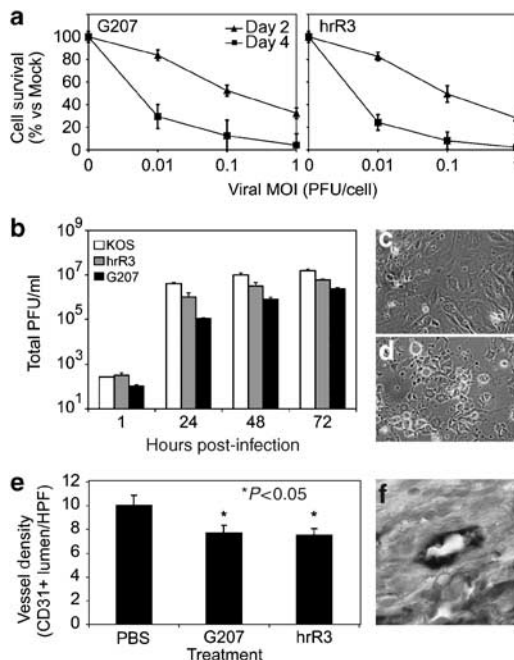


Figure 4 oHSV mutants are anti-angiogenic *in vitro* and *in vivo*. (a) Cytotoxicity assay showed potent oHSV effects against early passage, dividing endothelial cells (HUVECs) at 2 (▲) and 4 (■) days post-infection. (b) Virus replication assay in HUVECs infected by wild-type HSV-1 KOS (□), hrR3 (▨), and G207 (■) harvested at 1, 24, 48, and 72 h post-infection. (c) Mock infected or (d) G207-infected HUVECs (18 h post-infection) imaged by phase contrast microscopy (original magnification × 400). (e) Assessment of oHSV-mediated effects on tumor angiogenesis within MPNST xenografts. S.c. tumors were treated with a single injection of 5 × 10⁶ PFU oHSV and vessels were identified as CD31⁺ lumens per original magnification × 400 high power field. (f) Blood vessel from MPNST xenograft i.t. injected with hrR3 showing positive HSV immunostaining (original magnification × 400).

Erlotinib alters gene expression and inhibits growth of MPNST and endothelial cells

To assess the antitumor effects of erlotinib *in vitro*, we examined expression of proangiogenic genes, cell viability and tumor vessel density. Others have shown in a mesothelioma model that EGFR inhibition mediates a decrease in tumor angiogenesis by reduction of vascular endothelial growth factor²⁴ and matrix metalloproteases.²⁵ To test whether these pathways are affected by EGFR inhibition in MPNSTs, signaling through EGFR was inhibited with the small molecule EGFR tyrosine kinase inhibitor erlotinib. When grown in the presence of erlotinib, MPNST cell lines STS26T and S462 showed a reduced expression pattern of proangiogenic genes (Figure 5a) and demonstrated antiproliferative effects (Figure 5b). HUVECs grown in the presence of erlotinib also showed inhibited growth (Figure 5c). S.c. tumors treated with erlotinib daily, for five consecutive days, illustrated a reduction in vascular density (P<0.01) (Figure 5d) and analysis of vessel size distribution showed a trend toward decreased small vessels within erlotinib-treated tumors (data not shown). These results suggest that erlotinib has antiproliferative and antiangiogenic effects against MPNSTs.

The combination of oHSV and erlotinib enhances growth inhibition of MPNST cells

We reasoned that inhibition of EGFR in combination with oHSV might enhance anti-MPNST efficacy. When cultured in the presence of erlotinib, the MPNST cell line STS26T showed a

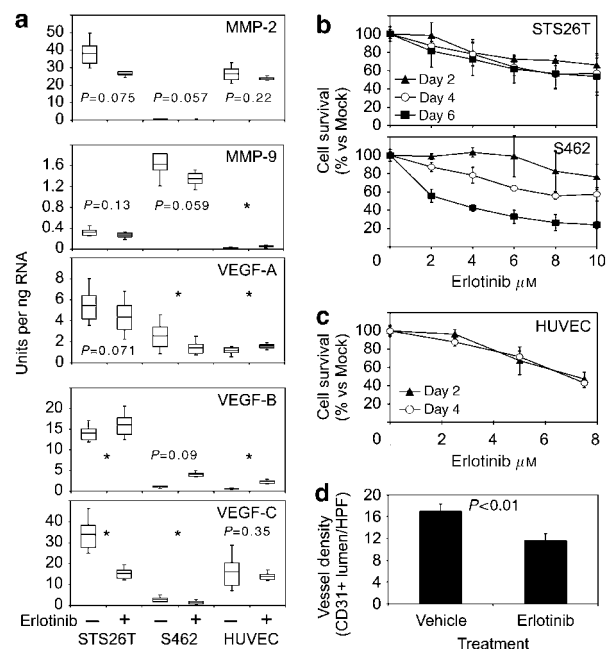


Figure 5 Erlotinib alters gene expression, MPNST cell proliferation and tumor angiogenesis. (a) RT-qPCR analysis of proangiogenic gene expression in MPNST cell lines and HUVECs grown in the absence or presence of erlotinib (*P<0.05). Cytotoxicity assay showing effect of erlotinib against (b) MPNST cell lines STS26T and S462 and (c) HUVEC at 2 (▲), 4 (○), and 6 (■) days post-infection. (d) Assessment of erlotinib-mediated effect on tumor angiogenesis within MPNST xenografts by quantification of CD31⁺ lumens per original magnification × 400 high power field.

significant reduction in EGFR phosphorylation (Figure 6a). STS26T cells treated with the combination of oHSV and erlotinib showed enhancement of cytotoxic effects at days 1, 2, and 4 post-infection (Figure 6b). We have previously documented the ability of MPNST cell lines to replicate oHSV mutants G207 and hrR3.¹³ To determine if EGFR signaling was required for replication of oHSV in MPNST cells, we examined virus replication in MPNST cell lines grown in the presence of erlotinib. oHSV replication was not altered in the presence of erlotinib, suggesting that EGFR activation is not necessary for robust virus replication (data not shown). Overall, our *in vitro* results suggest that the combination of erlotinib and oHSV is advantageous.

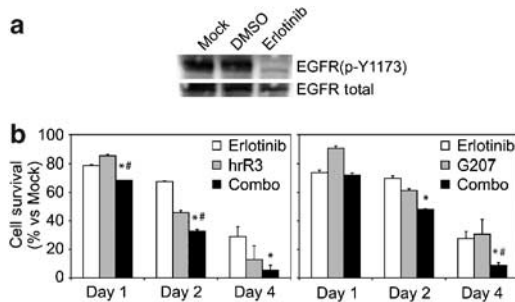


Figure 6 Combination of erlotinib and oHSV against MPNST cell lines in culture. (a) Protein extracts from STS26T cells treated with erlotinib, were separated by SDS-PAGE and immunoblotted with total EGFR and phospho-EGFR (Y-1173) antibodies. (b) Cytotoxicity assay showing effect of erlotinib alone (□), oHSV alone (■), and combination treatment (■) against MPNST cell line STS26T at days indicated post-infection (**P*<0.01 vs erlotinib alone, #*P*<0.01 vs virus alone).

Erlotinib and oHSV are efficacious against MPNST xenografts

To investigate the therapeutic potential of oHSV in combination with EGFR inhibition we coadministered these agents to tumor bearing mice. Animals received vehicle or erlotinib (25 mg/kg) by daily gavage with or without i.t. or i.p. injection of G207 or hrR3 (7.5×10^6 PFU/dose, total dose of 3×10^7 PFU) (Figure 7a). An additional group of mice bearing i.p. tumor burden received three doses of oHSV (1×10^7 PFU/dose, same total dose of 3×10^7 PFU) as in Figure 3 for comparison with the four dose regimen. By day 30, mice treated i.p. with four doses of PBS or UV-inactivated hrR3 appeared cachectic and had severe ascites. Erlotinib treatment alone showed a reduction in i.p. tumor nodule count (*P*<0.01) and a trend toward reduction in tumor weight (Figure 7b). All groups of mice treated with oHSV showed a dramatic reduction in number of tumor nodules and tumor weight (*P*<0.001). Combination treatments did not enhance the dominant antitumor oHSV effect. Comparison of the treatment regimens that split the total virus dose into four vs three fractions showed a slight improvement. Overall, oHSV and erlotinib were effective in reducing i.p. MPNST xenograft tumor burden.

Animals, bearing s.c. MPNST xenografts, that received UV-inactivated hrR3 showed rapid tumor growth. Whereas erlotinib-treated mice showed a modest growth reduction, oHSV-treated tumors showed a striking inhibition of tumor volume (*P*<0.00005) (Figure 7c). An additional cohort of mice was treated as above and followed for overall survival. In this experiment erlotinib alone showed a modest prolongation of median overall survival (*P*<0.12), whereas G207- or hrR3-treated mice showed impressive prolongation of survival by ~50 and ~90%, respectively (*P*<0.0001) (Figure 7d).

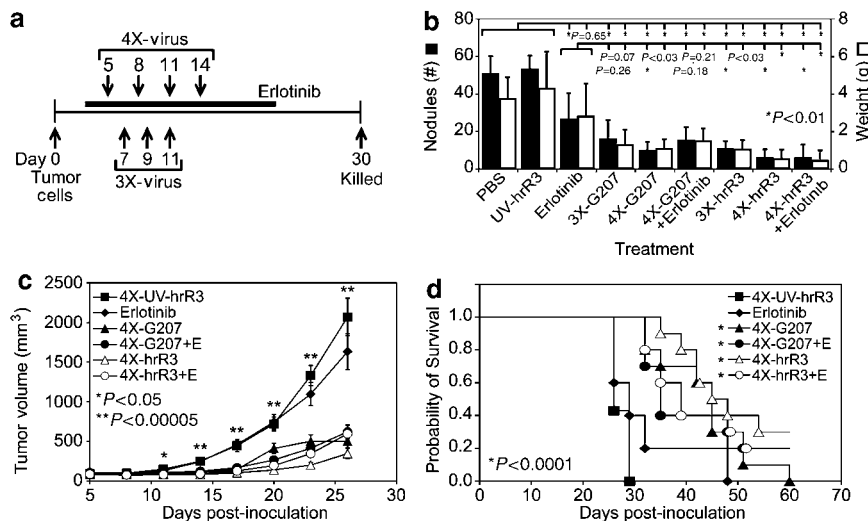


Figure 7 Treatment of MPNST xenografts with erlotinib and oHSV. (a) Treatment regimen indicating i.p. or s.c. injection with tumor cells, followed by treatment with virus split into 4 or 3 doses +/- 21 days of erlotinib by oral gavage. Evaluation of tumor burden at day 30 showing reduction of (b) tumor nodule count (■) and total tumor weight (□), standard deviation as shown (**P*<0.01). (c) Growth curves of s.c. MPNST xenografts treated with four doses of UV-inactivated hrR3 (■), erlotinib alone (◆), G207 (▲), G207 and erlotinib (●), hrR3 (△) or hrR3 and erlotinib (○), standard error as shown (**P*<0.05, ***P*<0.00005). (d) Overall survival of tumor bearing mice treated with four doses of UV-inactivated hrR3 (■), erlotinib alone (◆), G207 (▲), G207 and erlotinib (●), hrR3 (△) or hrR3 and erlotinib (○) (*log-rank *P*<0.0001).

DISCUSSION

We developed and utilized an MPNST xenograft models to evaluate the preclinical efficacy of oncolytic HSVs and the EGFR inhibitor, erlotinib. Animals treated with erlotinib alone exhibited a trend in tumor reduction but those treated with oHSV showed highly significant antitumor effects. I.p. delivery of oHSV was tumor selective, and MPNST xenografts supported replication of oHSV. Coadministration of oHSV and erlotinib *in vitro* demonstrated that inhibition of EGFR signaling did not adversely affect virus replication; in fact, overall cell killing was enhanced by the combination. Nevertheless, the potent anti-MPNST activity of oHSV was not enhanced by combination with erlotinib. Interestingly, both oHSVs and erlotinib exerted antiangiogenic effects. These data suggest that oHSVs inhibited tumor growth through multiple non-redundant mechanisms that were not diminished by combination with an EGFR inhibitor.

MPNSTs are relatively resistant to traditional anticancer therapies and require novel therapeutics, which have been hampered by a paucity of appropriate preclinical xenograft models.^{26,27} Using a human cell line derived from a sporadic case of MPNST, we developed s.c. and i.p. MPNST xenograft models that closely resemble human disease as measured by immunostaining and microarray analysis and that should prove useful for testing other experimental therapeutics. The advantage of these models over the existing model in NF1^{+/-}; p53^{+/-} (NP-*cis*) mice is that cells are of human origin, and therefore are most useful for testing biological therapeutics with human tropism such as antibodies and viruses. In addition, the model is reproducible and rapidly progressive, facilitating expedited testing of investigational therapeutics. Limitations of the xenograft models include the lack of T-cell immunity as well as the fact that the tumors are not an outgrowth of nerve sheaths, so the tumor microenvironment may not be authentic.

Owing to their cytostatic nature, inhibitors of signaling pathways key to MPNST pathogenesis such as erlotinib are unlikely to eradicate existing tumors. In addition, a drawback to treatments that target-specific signaling pathways is the development of mutations that confer resistance to tumor cell clones that are able to repopulate.²⁸ Thus, it is attractive to develop antitumor therapeutics that not only slow the growth of malignant tissue but also destroy the existing tumor and do not confer resistance.

Oncolytic HSVs are an exciting biological based anticancer therapeutic under development. Injection of oHSV into tumors causes reduction of tumor burden by multiple mechanisms, including direct cytotoxicity, stimulation of anti-tumor immune responses^{29,30} and inhibition of angiogenesis.^{22,23} There are no reports of initially sensitive tumor cell clones acquiring resistance to oHSV. The ability of oHSV to selectively target cells with hyperactive Ras signaling makes oHSV a highly rational candidate for treatment of NF1-associated malignancies. We have previously documented that human MPNST cell lines (both NF1-associated and sporadic) but not NHSC are permissive for productive oHSV infection.¹³ Our xenograft data confirm the sensitivity of MPNSTs to the effects of oHSV *in vivo*.

Both erlotinib and oHSVs had antiangiogenic effects in our models. Tumor-associated neoangiogenesis appears to play an important role in the pathogenesis of NF1-associated malignancies as haploinsufficiency of *NF1* augments angiogenesis,³¹⁻³³ and angiogenic factors including EGF, vascular endothelial growth factor, Midkine, platelet-derived growth factor and fibroblast growth factor-2 have been identified within neurofibromas.³⁴ Additionally, neurofibroma-derived Schwann cells display angiogenic and invasive properties,³⁵ and MPNSTs are known to be highly vascular. Thus, antiangiogenic properties of erlotinib and oHSV may play a role in their antitumor effects.

The fact that combination of oHSV with erlotinib did not show enhancement of the antitumor effect may be explained by a number of non-exclusive hypotheses. First, a higher dose of erlotinib may be required to observe any enhancement of the oHSV-mediated antitumor effect. Although some investigators have shown higher efficacy of erlotinib in non-MPNST preclinical models using higher doses,³⁶ in our experiments we chose to administer erlotinib at a clinically relevant dose of 25 mg/kg/day. This dose predicts a similar "area under the curve" (1,396 day-ng/mL in mice given 20 mg/kg/day) as that achievable in humans (1,520 day-ng/mL in humans given 150 mg daily).^{36,37} Another explanation for the lack of a combination effect could be that the dramatic antitumor effect of oHSV overshadowed the relatively modest erlotinib effect; therefore, administration of a lower dose of oHSV may reveal an additive effect of erlotinib. It is also possible that MPNST xenografts treated with erlotinib had acquired resistance to erlotinib or lost dependence upon EGFR signaling. In that case, other factors could bypass a need for EGFR-mediated signaling.

In conclusion, our preclinical results demonstrate robust anti-MPNST efficacy of oHSV, alone or in combination with erlotinib. Strategies to further enhance antitumor efficacy of oHSV include increasing virus spread,³⁸ placing ICP34.5 under a tumor-specific promoter³⁹ or insertion of antitumor/immunomodulatory transgenes into the viral genome.⁴⁰⁻⁴² As MPNSTs remain a significant clinical challenge, discovery of treatments for this disease is imperative. Overall, our results support continued investigation of attenuated oHSV mutants and erlotinib as possible treatments for MPNSTs.

MATERIALS AND METHODS

Cell culture and reagents. African green monkey kidney cells (Vero), rabbit skin cells and human MPNST cells have been previously described.¹³ Single donor HUVECs were cultured in EBM plus SingleQuots growth supplements media (Cambrex, Rockland, ME). HSV-1 (F) mutant G207 and HSV-1 (KOS) mutant hrR3 have been described.^{43,44} Both virus mutants possess the lacZ gene inserted into the *U_L39* locus and G207 contains a 1-kb deletion in both copies of the γ_1 34.5 gene. Viral stocks were propagated on Vero cells and titered on rabbit skin cells.¹³ Erlotinib (Tarceva[®], OSI-774), was provided by OSIS Pharmaceuticals (Melville, NY).

Microarray analysis of MPNST genes. Affymetrix MAS *.cel files from STS26T cell culture samples, STS26T xenograft tumors, NHSC samples, and 42 primary MPNST samples²¹ were imported into GeneSpring GX 7.3. Normalization of the data included RMA processing, followed by

per chip normalization to the median, and per gene normalization to the NHSC samples. Unsupervised hierarchical cluster analysis using Pearson Correlation for a distance metric was used to arrange the 159 genes in the MPNST signature according to similar expression patterns.

In vitro and in vivo virus replication assays. *In vitro:* Cells were plated in 12 well plates and infected with G207 or hrR3 at a multiplicity of infection = 0.1. After 2 h, cultures were washed twice with PBS and replenished with fresh media. When indicated, 10 μ M erlotinib or 0.1% dimethylsulfoxide was added to cultures 1 h before viral infection. Cultures were harvested and subjected to plaque assay on rabbit skin cells monolayers. *In vivo:* s.c. MPNST xenografts (~ 500 mm³) were injected with 5×10^6 PFU G207 or hrR3. Mice were euthanized at indicated times post-infection, tumors harvested, homogenized in PBS and subjected to plaque assay.

In vitro viral cytotoxicity assay. Tumor or HUVEC cells were plated in 96-well plates. Erlotinib, dimethylsulfoxide, G207, hrR3 or combinations were added and incubated at 37°C, 5% CO₂. Cultures were assessed for viable cells via the CellTiter96 kit (Promega, Madison, WI) as instructed.

RNA extraction, cDNA synthesis and quantitative RT-PCR analysis. RNA was extracted using Trizol (Invitrogen, Carlsbad, CA) followed by RNeasy (Qiagen, Valencia, CA). Two micrograms total RNA and 1 μ g oligo-dT (Invitrogen) were incubated at 70°C for 10 min. Four microliters 5X first-strand synthesis buffer (Invitrogen), 2 μ L 0.1 M dithiothreitol (Invitrogen), 0.5 μ L 0.1 M dNTP (Invitrogen), 0.5 μ L RNAguard (Amersham Biosciences, Piscataway, NJ), and 1 μ L M-MLV reverse transcriptase (Promega, Madison, WI) were added to the reaction, and incubated at 37°C for 1 h. The reaction was stopped by incubation at 70°C. One μ L of synthesized cDNA was combined with forward and reverse primers (5 pmol each) and 10 μ L of 2X DyNamo HS SYBR Green qPCR master mix (New England BioLabs, Ipswich, MA). Optimum annealing temperatures for each primer set was determined individually. RT-qPCR was performed in DNA Engine Opticon 2 Continuous Fluorescence Detection System (BioRad, Hercules, CA). Sample RNA was processed in triplicate with serial dilutions of Human Universal Reference RNA (Stratagene, La Jolla, CA) on the same 96-well plate. Standard curves were constructed from the Universal RNA wells with arbitrary units of 1 unit equivalent to 1 pg of Universal RNA. Specific genes were plotted as units/ng of RNA. Graphically, the middle line of the bar represents mean, bar size corresponds to the difference between lower quartile and upper quartile, and error bars represent the range of the raw data. Results were compared by *t*-test. Primers used as listed in **Supplementary Table S3**.

In vivo tumor models and treatments. Animal studies were approved by the Cincinnati Children's Hospital Medical Center Institutional Animal Care and Use Committee. Human MPNST cells ($1-2 \times 10^6$) in 30% Matrigel (BD Biosciences, San Diego, CA) were injected s.c., or ($3-4 \times 10^6$) in 750 μ L PBS were injected i.p., into 6- to 8-week-old female athymic nude (nu/nu) mice (Harlan, Indianapolis, IN), 8- to 10-week-old male and female non-obese diabetic and severe combined immunodeficient (NOD/SCID) mice (in house colony) or 8- to 10-week-old male and female NOD/SCID/ β 2-microglobulin^{-/-} (in house colony). Mice were evaluated for greater than four months for development of tumor burden.

Athymic nude mice were inoculated on day 0 with 4×10^6 STS26T cells by i.p. injection, and further administered i.p. injections of PBS, G207 or hrR3 ($1 \times 10^5-1 \times 10^7$ PFU/dose) on days 7, 9, and 11. Mice were euthanized and assessed for tumor burden at day 30 or followed for survival. Cell lines were established from harvested tumor specimens by mincing and incubating in $1 \times$ Liberase enzyme cocktail (Roche, Indianapolis, IN) and used in cytotoxicity assays before passage 4.

For combination efficacy studies, mice with s.c. tumors (100 mm³) were randomly separated into groups. Treatment groups consisted of vehicle 0.5% carboxymethyl-cellulose (Sigma, St Louis, MO) by daily gavage, 25 mg/kg erlotinib by daily gavage days 3–23, i.t. injection of hrR3, or G207 at a dose of 7.5×10^6 PFU on days 5, 8, 11, and 14 post-inoculation, or combinations of erlotinib plus i.t. virus injections. Erlotinib was prepared daily in 6% dimethylsulfoxide and 0.5% carboxymethyl-cellulose to a final concentration of 10 mg/mL. Tumor volumes were determined by $\text{Volume} = (\text{Length} \times \text{Width}^2) \times \pi/6$ and mice were euthanized when tumors reached 10% of the total body weight. As a control hrR3 was UV-inactivated in a Stratalink (Stratagene) at a wavelength of 254 nm for 10 min.

Biodistribution of oHSV following i.p. injection. I.p. MPNST xenograft tumors (16 days post-tumor cell injection) were treated with an injection of PBS or hrR3 (1×10^7 PFU) in 0.75 mL. At days 3 and 7 post-infection, mice were euthanized, tumor and organs harvested, homogenized and assayed for protein concentration and β -galactosidase activity as previously reported.¹³

IHC and in situ hybridization. Five μ m sections cut from formalin-fixed paraffin-embedded tumors were treated with 3% hydrogen peroxide in methanol for 10 min at room temperature followed by 0.1% trypsin (Gibco, Grand Island, NY) for epitope retrieval. Sections were protein blocked, incubated with the primary rat anti-CD31 antibody (BD Biosciences) at a 1:40 dilution for 60 min at room temperature, washed and treated with rabbit anti-rat secondary (Vector laboratories, Burlingame, CA) for 30 min. Detection was carried out via avidin-biotin complex for 30 min followed by incubation for 5 min with diaminobenzidine (DAKO, Carpinteria, CA) and haematoxylin counterstaining. Tumor vascular density was quantified via blinded counting of the mean number of vessels (identified by CD31⁺ staining around a lumen) within 10 high power fields ($\times 400$). IHC procedures included rehydration, heated epitope retrieval using Trilogy reagent (Cellmarque, Hot Springs, AR), endogenous peroxidase blocking and incubation with primary α -S100, α -synaptophysin, α -EGFR antibodies (DAKO), and α -HSV-1/2 antibody (Cellmarque). Signal was detected according to the DAKO Link+, Label+, DAB system. *In situ* hybridization for HSV genomes was performed according to the manufacturer's procedures using 2 μ L of HSV probe per slide (Enzo Biochem, New York, NY).

Denaturing electrophoresis and immunoblotting. Subconfluent STS26T cells were serum starved for 12 h and later supplemented with media containing 50 ng/mL EGF (Invitrogen) +/- erlotinib (10 μ M) or dimethylsulfoxide (0.1%). At 1 h, cells were washed twice with ice cold PBS and cell lysates were collected using M-PER protein collection buffer (Pierce, Rockford, IL) containing 50 mM NaF, 1 mM NaVO₃ and $1 \times$ protease inhibitor (Roche). Protein lysates were sonicated and submitted to ultra-centrifugation (18,000 $\times g$). Protein (30 μ g) was subjected to denaturing electrophoresis followed by electro-transfer to polyvinylidene fluoride membrane (Biorad). Primary anti-EGFR (1:5,000) and anti-Phospho-EGFR (p1173); (1:1,000) antibodies (Epitomics, Burlingame, CA) were incubated with blots at room temperature for 1 h. Blots were incubated with secondary anti-rabbit IgG HRP (Amersham Biosciences) and signal detection by Western lightening ECL reagent plus (Perkin-Elmer, Boston, MA).

Statistical analysis. Statistical analyses were performed by analysis of variance followed by means comparison using *post hoc* Tukey's tests and log-rank for survival studies using SPSS 12.0 software.

ACKNOWLEDGMENTS

Special thanks to Dr Sandra Weller (Department of Molecular, Microbial and Structural Biology, University of Connecticut) for providing hrR3, to MediGene for providing G207, to OSI Pharmaceuticals for providing erlotinib, to Dr Nancy Sawtell (Division of Infectious Diseases, Cincinnati Children's Hospital Medical Center) for providing wild-type HSV-1 KOS and RSCs, to Sharon Keys (Division of Veterinary Services, Cincinnati Children's Hospital Medical Center) for gavage assistance, to Betsy Dipasquale (Division of Pathology, Cincinnati Children's Hospital Medical Center) for IHC and *in situ* hybridization, to Yongchun Wu (Institute for Genetic Medicine, University of Southern California) for statistical analysis of RT-PCR data, to Dr Arturo Maldonado (Division of Pediatric General, Thoracic and Fetal Surgery, Cincinnati Children's Hospital Medical Center), Jennifer Leddon, William Baird and Greg Kottyan (all Physician Scientist Training Program, University of Cincinnati College of Medicine) for manuscript review. This work was supported by Cincinnati Children's Hospital Medical Center Division of Hematology and Oncology, TeeOffAgainstCancer.org, the Sara Zepernick Foundation and NIH grant R01-CA114004.

SUPPLEMENTARY MATERIAL

Table S1. Tumor formation in immunodeficient mice following subcutaneous and intraperitoneal injection of human MPNST cell lines.

Table S2. Genes dysregulated in MPNSTs and xenograft model.

Table S3. Primers used for real time RT-PCR.

REFERENCES

- Theos, A and Korf, BR (2006). Pathophysiology of neurofibromatosis type 1. *Ann Intern Med* **144**: 842-849.
- Evans, DG, Baser, ME, McGaughran, J, Sharif, S, Howard, E and Moran, A (2002). Malignant peripheral nerve sheath tumours in neurofibromatosis 1. *J Med Genet* **39**: 311-314.
- Sharif, S *et al.* (2006). Second primary tumors in neurofibromatosis 1 patients treated for optic glioma: substantial risks after radiotherapy. *J Clin Oncol* **24**: 2570-2575.
- Basu, TN, Gutmann, DH, Fletcher, JA, Glover, TW, Collins, FS and Downward, J (1992). Aberrant regulation of ras proteins in malignant tumour cells from type 1 neurofibromatosis patients. *Nature* **356**: 663-664.
- DeClue, JE *et al.* (2000). Epidermal growth factor receptor expression in neurofibromatosis type 1-related tumors and NF1 animal models. *J Clin Invest* **105**: 1233-1241.
- Aghi, M and Martuza, RL (2005). Oncolytic viral therapies—the clinical experience. *Oncogene* **24**: 7802-7816.
- Currier, M, Mahller, Y, Adams, L and Cripe, T (2005). Widespread intratumoral virus distribution with fractionated injection enables local control of large human rhabdomyosarcoma xenografts by oncolytic herpes simplex viruses. *Cancer Gene Ther* **12**: 407-416.
- Pawlik, TM *et al.* (2000). Oncolysis of diffuse hepatocellular carcinoma by intravascular administration of a replication-competent, genetically engineered herpesvirus. *Cancer Res* **60**: 2790-2795.
- Parikh, N *et al.* (2005). Oncolytic herpes simplex virus mutants are more efficacious than wild-type adenovirus for the treatment of high-risk neuroblastomas in preclinical models. *Pediatric Blood Cancer* **44**: 469-478.
- Shen, Y and Nemunaitis, J (2006). Herpes simplex virus 1 (HSV-1) for cancer treatment. *Cancer Gene Ther* **7**: 7.
- Farassati, F, Yang, AD and Lee, PW (2001). Oncogenes in Ras signalling pathway dictate host-cell permissiveness to herpes simplex virus 1. *Nat Cell Biol* **3**: 745-750.
- Sarinella, F, Calistri, A, Sette, P, Palu, G and Parolin, C (2006). Oncolysis of pancreatic tumour cells by a gamma34.5-deleted HSV-1 does not rely upon Ras-activation, but on the PI 3-kinase pathway. *Gene Ther* **23**: 23.
- Mahller, YY, Rangwala, F, Ratner, N and Cripe, TP (2006). Malignant peripheral nerve sheath tumors with high and low Ras-GTP are permissive for oncolytic herpes simplex virus mutants. *Pediatr Blood Cancer* **46**: 745-754.
- Mendelsohn, J and Baselga, J (2003). Status of epidermal growth factor receptor antagonists in the biology and treatment of cancer. *J Clin Oncol* **21**: 2787-2799.
- Phillip, PA *et al.* (2005). Phase II study of erlotinib (OSI-774) in patients with advanced hepatocellular cancer. *J Clin Oncol* **23**: 6657-6663.
- Haas-Kogan, DA *et al.* (2005). Epidermal growth factor receptor, protein kinase B/Akt, and glioma response to erlotinib. *J Natl Cancer Inst* **97**: 880-887.
- Hainsworth, JD, Sosman, JA, Spigel, DR, Edwards, DL, Baughman, C and Greco, A (2005). Treatment of metastatic renal cell carcinoma with a combination of bevacizumab and erlotinib. *J Clin Oncol* **23**: 7889-7896.
- Shepherd, FA *et al.* (2005). Erlotinib in previously treated non-small-cell lung cancer. *N Engl J Med* **353**: 123-132.
- Soulieres, D, Senzer, NN, Vokes, EE, Hidalgo, M, Agarwala, SS and Siu, LL (2004). Multicenter phase II study of erlotinib, an oral epidermal growth factor receptor tyrosine kinase inhibitor, in patients with recurrent or metastatic squamous cell cancer of the head and neck. *J Clin Oncol* **22**: 77-85.
- Albritton, KH *et al.* (2006). Phase II study of erlotinib in metastatic or unresectable malignant peripheral nerve sheath tumors (MPNST). *J Clin Oncol* **24**, abs. 9518.
- Miller, SJ *et al.* (2006). Large-scale molecular comparison of human schwann cells to malignant peripheral nerve sheath tumor cell lines and tissues. *Cancer Res* **66**: 2584-2591.
- Cinatl Jr, J *et al.* (2004). Multimutated herpes simplex virus g207 is a potent inhibitor of angiogenesis. *Neoplasia* **6**: 725-735.
- Benencia, F *et al.* (2005). Oncolytic HSV exerts direct antiangiogenic activity in ovarian carcinoma. *Hum Gene Ther* **16**: 765-778.
- Sini, P *et al.* (2005). The antitumor and antiangiogenic activity of vascular endothelial growth factor receptor inhibition is potentiated by ErbB1 blockade. *Clin Cancer Res* **11**: 4521-4532.
- Liu, Z and Klominek, J (2004). Inhibition of proliferation, migration, and matrix metalloprotease production in malignant mesothelioma cells by tyrosine kinase inhibitors. *Neoplasia* **6**: 705-712.
- Hirokawa, Y *et al.* (2005). Signal therapy of NF1-deficient tumor xenograft in mice by the anti-PAK1 drug FK228. *Cancer Biol Ther* **4**: 379-381.
- Ratner, N and Miller, SJ (2006). Model systems for neurofibroma and malignant peripheral nerve sheath tumors. *Drug Discov Today* **3**: 175-182.
- Pao, W *et al.* (2005). Acquired resistance of lung adenocarcinomas to gefitinib or erlotinib is associated with a second mutation in the EGFR kinase domain. *PLoS Med* **2**: e73.
- Jarnagin, WR *et al.* (2003). Neoadjuvant treatment of hepatic malignancy: an oncolytic herpes simplex virus expressing IL-12 effectively treats the parent tumor and protects against recurrence after resection. *Cancer Gene Ther* **10**: 215-223.
- Toda, M, Martuza, RL, Kojima, H and Rabkin, SD (1998). *In situ* cancer vaccination: an IL-12 defective vector/replication-competent herpes simplex virus combination induces local and systemic antitumor activity. *J Immunol* **160**: 4457-4464.
- Wu, M, Wallace, MR and Muir, D (2006). Nf1 haploinsufficiency augments angiogenesis. *Oncogene* **25**: 2297-2303.
- Ozerdem, U (2004). Targeting neovascular pericytes in neurofibromatosis type 1. *Angiogenesis* **7**: 307-311.
- Gitler, AD *et al.* (2003). NF1 has an essential role in endothelial cells. *Nat Genet* **33**: 75-79.
- Kurtz, A and Martuza, RL (2002). Antiangiogenesis in neurofibromatosis 1. *J Child Neurol* **17**: 578-584, discussion 602-574, 646-551.
- Sheela, S, Riccardi, VM and Ratner, N (1990). Angiogenic and invasive properties of neurofibroma Schwann cells. *J Cell Biol* **111**: 645-653.
- Higgins, B *et al.* (2004). Antitumor activity of erlotinib (OSI-774, Tarceva) alone or in combination in human non-small cell lung cancer tumor xenograft models. *Anticancer Drugs* **15**: 503-512.
- Herbst, RS *et al.* (2005). Phase I/II trial evaluating the anti-vascular endothelial growth factor monoclonal antibody bevacizumab in combination with the HER-1/epidermal growth factor receptor tyrosine kinase inhibitor erlotinib for patients with recurrent non-small-cell lung cancer. *J Clin Oncol* **23**: 2544-2555.
- McKee, TD *et al.* (2006). Degradation of fibrillar collagen in a human melanoma xenograft improves the efficacy of an oncolytic herpes simplex virus vector. *Cancer Res* **66**: 2509-2513.
- Kambara, H, Okano, H, Chiocca, EA and Saeki, Y (2005). An oncolytic HSV-1 mutant expressing ICP34.5 under control of a nestin promoter increases survival of animals even when symptomatic from a brain tumor. *Cancer Res* **65**: 2832-2839.
- Aghi, M, Chou, TC, Suling, K, Breakfield, XO and Chiocca, EA (1999). Multimodal cancer treatment mediated by a replicating oncolytic virus that delivers the oxazaphosphorine/rat cytochrome P450 2B1 and ganciclovir/herpes simplex virus thymidine kinase gene therapies. *Cancer Res* **59**: 3861-3865.
- Bennett, JJ *et al.* (2001). Interleukin 12 secretion enhances antitumor efficacy of oncolytic herpes simplex viral therapy for colorectal cancer. *Ann Surg* **233**: 819-826.
- Toda, M, Martuza, RL and Rabkin, SD (2000). Tumor growth inhibition by intratumoral inoculation of defective herpes simplex virus vectors expressing granulocyte-macrophage colony-stimulating factor. *Mol Ther* **2**: 324-329.
- Mineta, T, Rabkin, SD, Yazaki, T, Hunter, WD and Martuza, RL (1995). Attenuated multi-mutated herpes simplex virus-1 for the treatment of malignant gliomas. *Nat Med* **1**: 938-943.
- Goldstein, D and Weller, S (1988). Herpes simplex virus type 1-induced ribonucleotide reductase activity is dispensable for virus growth and DNA synthesis: isolation and characterization of an ICP6 lacZ insertion mutant. *J Virol* **62**: 196-205.